JPE 17-5-8

https://doi.org/10.6113/JPE.2017.17.5.1203
ISSN(Print): 1598-2092 / ISSN(Online): 2093-4718

Optimal Voltage Vector Selection Method for Torque Ripple Reduction in the Direct Torque Control of Five-phase Induction Motors

Seong-Yun Kang*, Hye Ung Shin**, Sung-Min Park***, and Kyo-Beum Lee†

*Dawonsys Co., Ltd, Ansan, Korea
**Department of Electric Powertrain R&D, Ssangyong Motor, Pyeongtaek, Korea
***Department of Electronic and Electrical Engineering, Hongik University, Sejong, Korea
†Department of Electrical and Computer Engineering, Ajou University, Suwon, Korea

Abstract

This paper presents an improved switching selection method for the direct torque control (DTC) of five-phase induction motors (IMs). The proposed method is conducted using optimal switching selection. A five-phase inverter has 32 voltage vectors which are divided into 30 nonzero voltage vectors and two zero voltage vectors. The magnitudes of the voltage vectors consist of large, medium, and small voltage vectors. In addition, these vectors are related to the torque response and torque ripple. When a large voltage vector is selected in a drive system, the torque response time decreases with an increased torque ripple. On the other hand, when a small voltage vector is selected, the torque response time and torque ripple increase. As a result, this paper proposes an optimal voltage vector selection method for improved DTC of a five-phase induction machine depending on the situation. Simulation and experimental results verify the effectiveness of the proposed control algorithm.

Key words: Five-phase inverter, Induction motor, Switching selection method, Voltage vector

I. INTRODUCTION

A five-phase induction motor (IM) has many merits when compared with three-phase induction motors. First, a five-phase IM has concentrated windings instead of sinusoidal windings. It generates at least 10% more output torque when compared with a three-phase IM [1]-[3]. Second, a five-phase IM has more voltage vectors when compared with a three-phase IM. Consequently, a five-phase IM is good for direct torque control (DTC) because it is possible to choose an optimal voltage vector for DTC.

DTC has many advantages, such as a fast torque response, a simple control method without a coordinate transformation, robustness against motor parameter variations, and a high-power motor drive method [4]-[14]. Because DTC is used with a chosen voltage vector, many voltage vectors are able to operate efficiently. Therefore, a five-phase IM is more efficient under DTC when compared with a three-phase IM [15]-[18].

However, DTC has drawbacks. A large torque ripple is generated in a low speed range because of the small back EMF of an induction machine. In addition, a short control period is required to achieve good performance, because DTC is performed by using a selected voltage vector during one control period. If the control period is long, torque ripple is produced by the applied effective voltage vector. Torque ripple reduction methods of DTC have been researched in [19]-[22]. Some of them have introduced a torque ripple reduction method for an interior permanent magnet synchronous motor (IPMSM). In addition, the other papers suggest methods to choose the optimal voltage vector selection method for the DTC of a five-phase IM [23], [24]. Depending on the magnitude of the voltage vector in a five-phase inverter, the torque and flux hysteresis bands using the DTC of five-levels are controlled by two different voltage vector magnitudes (large and medium voltage vectors) [23]. The hysteresis band in the case of seven levels is controlled by using all of the voltage vectors in a five-phase IM [24]. However, the look-up

Manuscript received Sep. 13, 2016; accepted Mar. 23, 2017
Recommended for publication by Associate Editor Gaolin Wang.
†Corresponding Author: kyl@ajou.ac.kr
Tel: +82-31-219-2376, Fax: +82-31-212-9531, Ajou University
*Dawonsys Co., Ltd, Korea
**Dept. of Electric Powertrain R&D, Ssangyong Motor, Korea
***Hongik University, Sejong, Korea

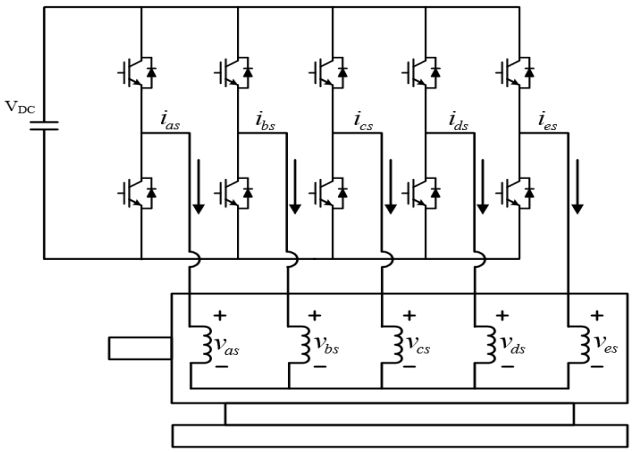

Fig. 1. Two-level inverter circuit for operating a five-phase IM.

V_{L1}[11001], V_{L2}[11000]	V_{M1}[10000], V_{M2}[11101]	V_{S1}[01001], V_{S2}[11010]
V_{L3}[11100], V_{L4}[01100]	V_{M3}[01000], V_{M4}[11110]	V_{S3}[10100], V_{S4}[01101]
V_{L5}[01110], V_{L6}[00110]	V_{M5}[00100], V_{M6}[01111]	V_{S5}[01010], V_{S6}[10110]
V_{L7}[00111], V_{L8}[00011]	V_{M7}[00010], V_{M8}[10111]	V_{S7}[00101], V_{S8}[01011]
V_{L9}[10011], V_{L10}[10001]	V_{M9}[00001], V_{M10}[11011]	V_{S9}[10010], V_{S10}[10101]
<Large Vector>	<Medium Vector>	<Small Vector>
< V_S: 0.6472 V_{DC} >	< V_S: 0.4 V_{DC} >	< V_S: 0.2472 V_{DC} >

Fig. 2. Switching state in a five-phase inverter.

table for the voltage vector selection provided by [23], [24] has a large voltage vector magnitude in the steady state. As a result, the selection of a large voltage vector does not facilitate torque ripple reduction.

This paper proposes an improved method for the voltage vector selection in a five-phase IM for DTC. The voltage vectors of a five-phase IM are composed of nonzero voltage vectors, which consist of a large voltage vector, a medium voltage vector, and a small voltage vector. The large voltage vector has a fast torque response in the transient state. However, if the large voltage vector is selected, the steady-state torque ripple increases in the low-speed area. As a result, in order to reduce the torque ripple, medium and small voltage vectors are used in the steady state. In addition, a large voltage vector is only used in the transient state. The proposed control strategy is verified by simulation and experiment results.

II. Improved Switching Selection Method

A. Voltage Vectors of a Five-Phase Inverter

A schematic of a five-phase IM drive is shown in Fig. 1. This paper uses a two-level inverter to operate a five-phase IM. The five-phase inverter is composed of two switches in each leg, which are operated complementarily. The voltage vectors of the five-phase inverter are composed of 32 voltage vectors. The switching states consist of two-zero voltage vectors and 30 nonzero voltage vectors.

Formulas for the phase and magnitude values of the voltage

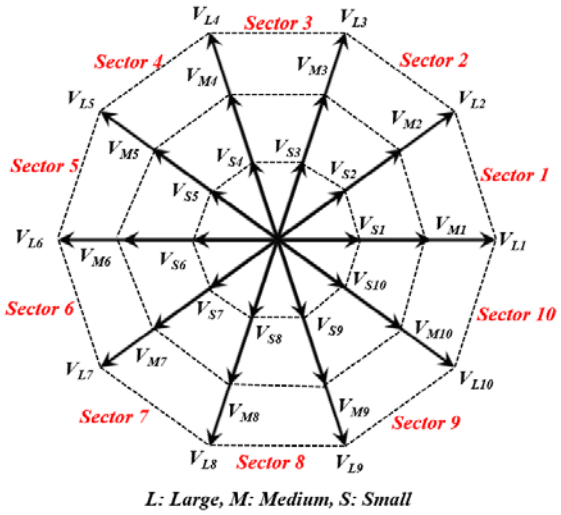

Fig. 3. Space vector plane in a five-phase VSI.

TABLE I
Proposed Lookup Table for Voltage Vector Selection

C_F	C_T	Sector Number									
		1	2	3	4	5	6	7	8	9	10
+1	+3	V_{L3}	V_{L4}	V_{L5}	V_{L6}	V_{L7}	V_{L8}	V_{L9}	V_{L10}	V_{L1}	V_{L2}
	+2	V_{M3}	V_{M4}	V_{M5}	V_{M6}	V_{M7}	V_{M8}	V_{M9}	V_{M10}	V_{M1}	V_{M2}
	+1	V_{S3}	V_{S4}	V_{S5}	V_{S6}	V_{S7}	V_{S8}	V_{S9}	V_{S10}	V_{S1}	V_{S2}
	-1	V_{S9}	V_{S10}	V_{S1}	V_{S2}	V_{S3}	V_{S4}	V_{S5}	V_{S6}	V_{S7}	V_{S8}
	-2	V_{M9}	V_{M10}	V_{M1}	V_{M2}	V_{M3}	V_{M4}	V_{M5}	V_{M6}	V_{M7}	V_{M8}
	-3	V_{L9}	V_{L10}	V_{L1}	V_{L2}	V_{L3}	V_{L4}	V_{L5}	V_{L6}	V_{L7}	V_{L8}
-1	+3	V_{L4}	V_{L5}	V_{L6}	V_{L7}	V_{L8}	V_{L9}	V_{L10}	V_{L1}	V_{L2}	V_{L3}
	+2	V_{M4}	V_{M5}	V_{M6}	V_{M7}	V_{M8}	V_{M9}	V_{M10}	V_{M1}	V_{M2}	V_{M3}
	+1	V_{S4}	V_{S5}	V_{S6}	V_{S7}	V_{S8}	V_{S9}	V_{S10}	V_{S1}	V_{S2}	V_{S3}
	-1	V_{S8}	V_{S9}	V_{S10}	V_{S1}	V_{S2}	V_{S3}	V_{S4}	V_{S5}	V_{S6}	V_{S7}
	-2	V_{M8}	V_{M9}	V_{M10}	V_{M1}	V_{M2}	V_{M3}	V_{M4}	V_{M5}	V_{M6}	V_{M7}
	-3	V_{L8}	V_{L9}	V_{L10}	V_{L1}	V_{L2}	V_{L3}	V_{L4}	V_{L5}	V_{L6}	V_{L7}

vectors are:

$$\frac{2}{5}(S_a + aS_b + a^2 S_c + a^3 S_d + a^4 S_e) = f^s_{ds1} + jf^s_{qs1}, \quad (a = e^{j2\pi/5}) \tag{1}$$

$$\theta_{ph} = \tan^{-1}\left(\frac{f^s_{qs1}}{f^s_{ds1}}\right), \tag{2}$$

where, f^s_{ds1} and f^s_{qs1} are the dq-axis stationary reference frame voltage vectors by the switching state, and θ_{ph} is the phase angle. The magnitude of the voltage vectors is presented using (1) in Fig. 2. $V_{xy}[S_a\ S_b\ S_c\ S_d\ S_e]$ represents the switching state of the five-phase inverter in Fig. 2. Where, x is the large, medium, and small magnitude. y is the number of sector intervals according to the phase angle. S_a presents the switching state of the upper switch of phase A. For example, if the upper switch

of phase A is turned on, S_a becomes 1. The voltage vector magnitudes are divided into three categories: 0.6472 V_{DC} (the value of the large voltage vector), 0.4 V_{DC} (the value of the medium voltage vector), and 0.2472 V_{DC} (the value of the small voltage vector) [25]. The voltage vector plane of the five-phase IM is shown in Fig. 3. The voltage vector plane is represented using the voltage vector phase and magnitude. The large, medium, and small voltage vectors are placed at the same phase region. The phase angle of V_{L1}, V_{M1}, and V_{S1} is 0° by using (2). In addition, each voltage vector is divided by intervals of 36° according to the sector. It should be noted that the torque ripple and torque response speed can change in accordance with three voltage vectors of different magnitudes. Therefore, these vectors can be used to reduce the torque ripple for a five-phase IM.

B. Proposed Switching Selection Method

An optimal switching selection method is introduced by using the voltage vectors of a five-phase inverter. In order to control the flux and torque, the voltage vectors are selected from the hysteresis comparator output of the torque and flux [26].

The rotor flux formula is:

$$v_{dqs}^{s} = R_s i_{dqs}^{s} + \frac{d\lambda_{dqs}^{s}}{dt},\ \lambda_{dqs}^{s} = \int (v_{dqs}^{s} - R_s i_{dqs}^{s})dt, \quad (3)$$

$$\lambda_{dqr}^{s} = \frac{L_r}{L_m}(\lambda_{dqs}^{s} - \sigma L_s i_{dqs}^{s}),\ \theta_e = \tan^{-1}(\frac{\lambda_{qr}^{s}}{\lambda_{dr}^{s}}), \quad (4)$$

where, v^s_{dqs}, R_s, i^s_{dqs}, λ^s_{dqs}, λ^s_{dqr}, σ, L_s, L_r, L_m, and θ_e indicate the dq-axis voltage of the synchronous reference frame, stator resistance, stator dq-axis current, stator synchronous reference frame flux, rotor synchronous reference frame flux, leakage flux, stator inductance, rotor inductance, mutual inductance, and flux angle, respectively. The voltage model is used for calculating the flux angle and rotor flux, since it is a convenient flux estimator for IM control. Some motor parameters are needed to use the voltage model. Using (3) and (4), the estimated flux angle can be divided into 10 sectors of 36° each. After that, the voltage vector is selected by considering the output of the comparator and the estimated flux angle.

The proposed voltage vector selection for DTC is summarized as shown in Table I. In addition, the medium and small voltage vectors used in the steady state are indicated in the table. The large voltage vector is used in the transient state according to the proposed algorithm. C_T and C_F present the output values of the torque and flux comparator [27]. If C_T is +2 and -2, the medium voltage vector is selected. If C_T is +1 and -1, the small voltage vector is selected.

Fig. 4 shows the output torque using each of the voltage vectors in the five-phase inverter system. Fig. 4(a) presents the output torque in a short control period. The torque is controlled in the hysteresis band. On the other hand, Fig. 4(b) has a long control period. When a large voltage vector is selected during a

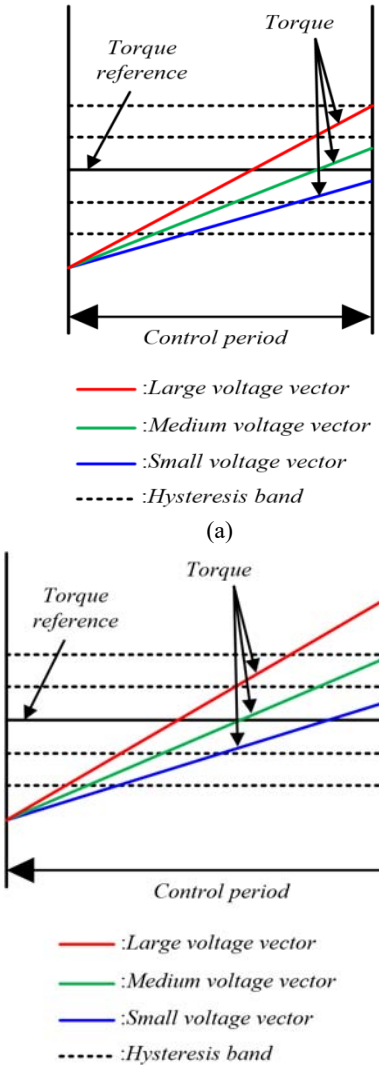

Fig. 4. Output torque using each of the voltage vectors in a five-phase inverter system. (a) Short control period. (b) Long control period.

long control period, the torque is controlled over the hysteresis band in each control time. As a result, a large torque is produced band in each control time. As a result, a large torque is produced by the large voltage vector. When a small voltage vector is selected at the same time, a small torque is produced by the small voltage vector. If the look-up table has a large voltage vector for the DTC, the torque ripple increases in a long control period and steady state. The large voltage vector is not used in the look-up table of the proposed method. Therefore, the torque ripple is reduced when compared to the conventional method. In addition, the proposed method has good performance in the low speed area where a large voltage vector is not required.

In order to reduce the torque ripple in the transient state, Fig. 5 shows the proposed selection method of a large voltage in the transient state. At first, this method can be verified using the difference of T_{ref}(k-1) and T_{ref}(k). Second, if the difference

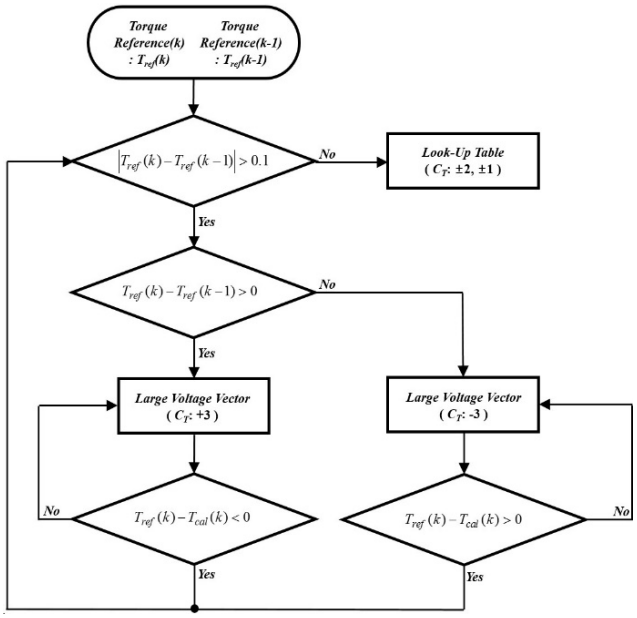

Fig. 5. Proposed large voltage vector selection method for a transient state.

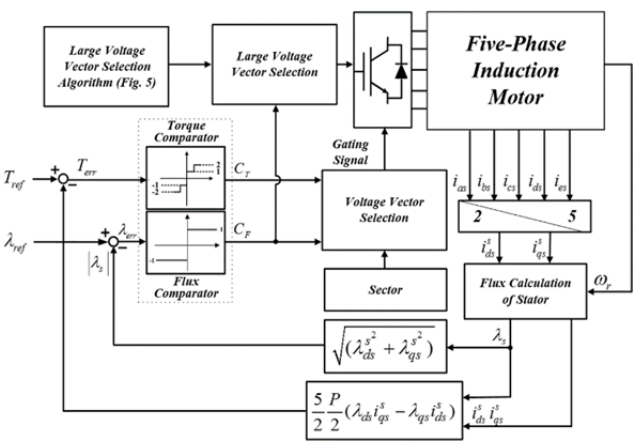

Fig. 6. Control block diagram of the proposed voltage vector selection method.

between T_{ref} (k-1) and T_{ref} (k) is bigger than 0.1 for the threshold, this situation becomes a transient state. Then a large voltage vector (C_T: +3 or -3) is selected in accordance with the difference between the torque references. After that, the next voltage vector is selected in accordance with the difference between T_{ref}(k) and T_{cal}(k). On the other hand, when it is less than 0.1, this situation becomes a steady state. After that, small and medium voltage vector (C_T: ±1, ±2) are selected using the magnitude of T_{ref} which can be divided into hysteresis bands. For example, when the torque reference is changed from 3 Nm to 5 Nm, T_{ref} (k-1) and T_{ref} (k) are 3 Nm and 5 Nm in the proposed method. Moreover, when T_{ref}(k-1) and T_{ref} (k) are not equal, a large voltage vector is selected.

Fig. 6 shows a control block diagram of the proposed voltage vector selection method. A transient state is used for the large voltage vector as shown in Fig. 5. In addition, small and medium voltage vectors are used for the steady state.

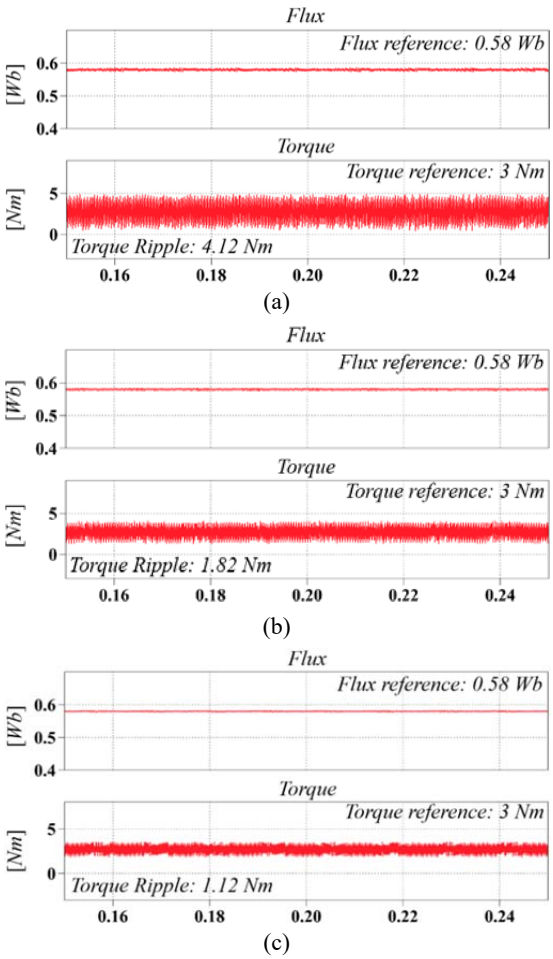

Fig. 7. Torque and flux control using different voltage vector magnitudes. (a) Large voltage vector. (b) Medium voltage vector. (c) Small voltage vector.

Therefore, when Fig. 6 is used in the five-phase inverter, the torque ripple can be reduced when compared with the conventional method.

III. Simulation Results

Simulation results are used to verify the optimal voltage vector selection method. The control time of the proposed method for the simulation is set to 100 μs. Furthermore, the speed is set to 300 rpm, the torque reference is set to 5 Nm, and the reference of the rated flux is 0.4 Wb in the PLECS tool.

Simulation results of the torque and flux control using different voltage vectors are shown Fig. 7. First, Fig. 7(a) shows the torque ripple when the DTC uses a large voltage vector. It has a torque ripple value of 3.07 Nm. The simulation result in the case of a small voltage vector is represented in Fig. 7(c).

As a result, when a small voltage vector is used for DTC, the torque ripple is 1.16 Nm, which is a reduction of approximately 1.19 Nm when compared with the case of a large voltage vector. In the steady state, the torque ripple has a minimum value when using a small voltage vector.

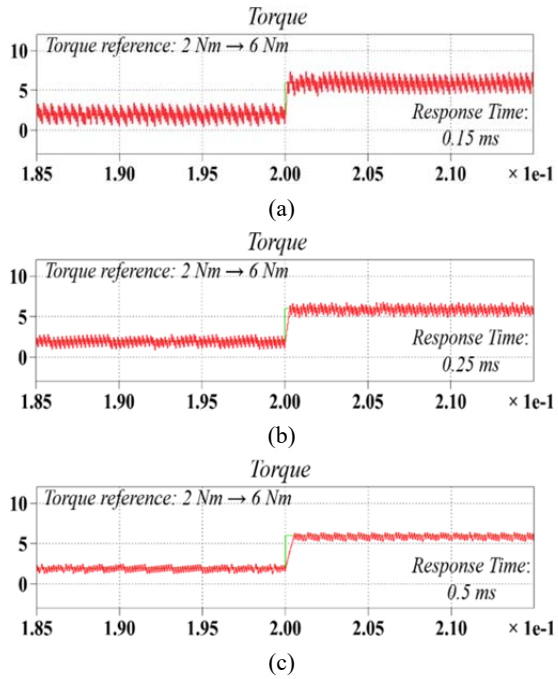

Fig. 8. Change in the torque reference (2 Nm → 6 Nm). (a) Large voltage vector. (b) Medium voltage vector. (c) Small voltage vector.

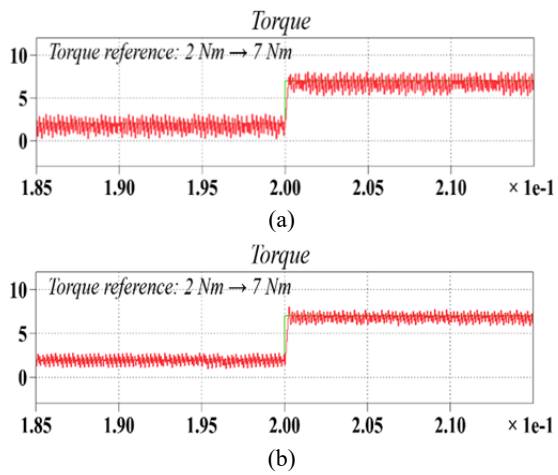

Fig. 9. Change in the torque reference (2 Nm → 7 Nm): (a) seven-level hysteresis band; (b) proposed method.

Fig. 8 shows simulation results of the DTC method for each of the voltage vectors in a transient state. At 0.2 s, the torque reference is changed from 2 Nm to 6 Nm. When a large voltage vector is selected for the DTC in a five-phase inverter, the time of the torque response is 0.15 ms in the transient state. On the other hand, when a small voltage vector is selected, the torque response time is 0.5 ms in the transient state. This means that the large voltage vector has the best performance considering the torque response time in a transient state owing to a maximum voltage input.

Comparison results of the seven-level comparator method and the proposed method are shown in Fig. 9. The torque response time of Fig. 9(a) is equal to that of Fig. 9(b) in the transient state because both methods use large voltage vectors. However, the torque ripple of Fig. 9(a) is larger than that of Fig. 9(b) because a large voltage vector is being used in both the transient state and the steady state in Fig. 9(a). The proposed method is controlled by a medium voltage vector and a small voltage vector (C_T: +2, +1, -1, -2) in the steady state. Therefore, the torque ripple of Fig. 9(b) is reduced in the steady state using the proposed method.

TABLE II
COMPARISON RESULTS OF THE VOLTAGE VECTORS

Comparison results / Voltage vector	Torque ripple	Response time
Large voltage vector	4.12 Nm	0.15 ms
Medium voltage vector	1.82 Nm	0.25 ms
Small voltage vector	1.12 Nm	0.5 ms

TABLE III
SPECIFICATIONS OF A FIVE-PHASE IM

Parameter	Value
Capacity	1.5 kW
Rated voltage	220 V
Rated frequency	60 Hz
Rated current	4.9 A
Rated speed	1684 rpm

Table II shows the torque ripple and torque response time using each of the voltage vectors. It is noted that a large voltage vector produces a large torque ripple. However, the torque response time is fast. In addition, a small voltage vector produces a small torque ripple. However, the torque response time is slow. Therefore, if a large vector is used only in the transient state, the torque ripple is reduced and the torque response is fast.

IV. EXPERIMENT RESULTS

The motor specifications are listed in Table III. The experimental setup consists of a load motor, a five-phase IM, a control board, and a power board, as shown in Fig. 10. A DSP controller, TMS320F 28335 from Texas Instruments, is used for the digital implementation of the proposed technique. The sampling time of the digital controller in the experimental setup is set to 100 μs.

Fig. 11 illustrates experimental results for different voltage vectors. The parameters are as follows: 3 Nm torque, 0.58 Wb flux, and 300 rpm speed. The case of a large voltage vector is shown in Fig. 11(a). It is clear that the torque ripple value is approximately 2.58 Nm. For a small voltage vector, the torque ripple is much smaller, with a value of 1.28 Nm. Therefore, the torque ripple decreases when using a small voltage vector.

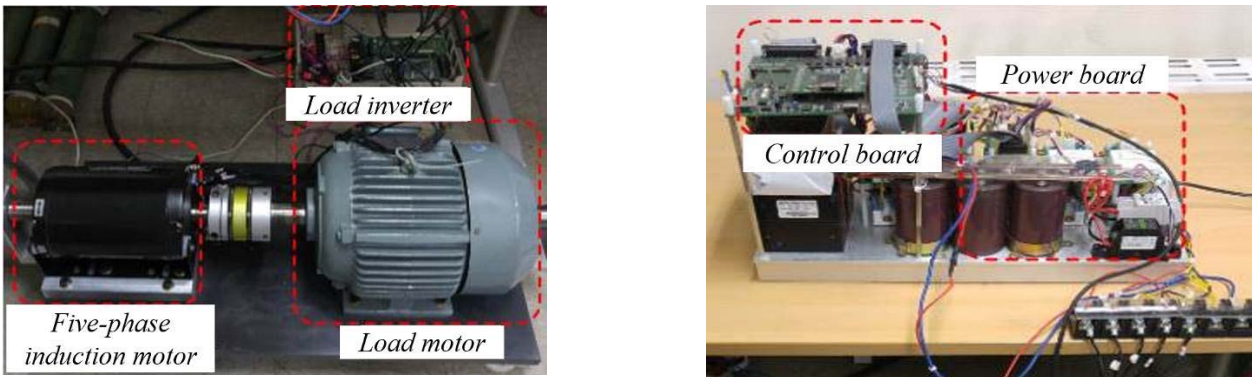

(a) (b)

Fig. 10. Experimental setup. (a) Five-phase IM and load motor. (b) Control board and power board.

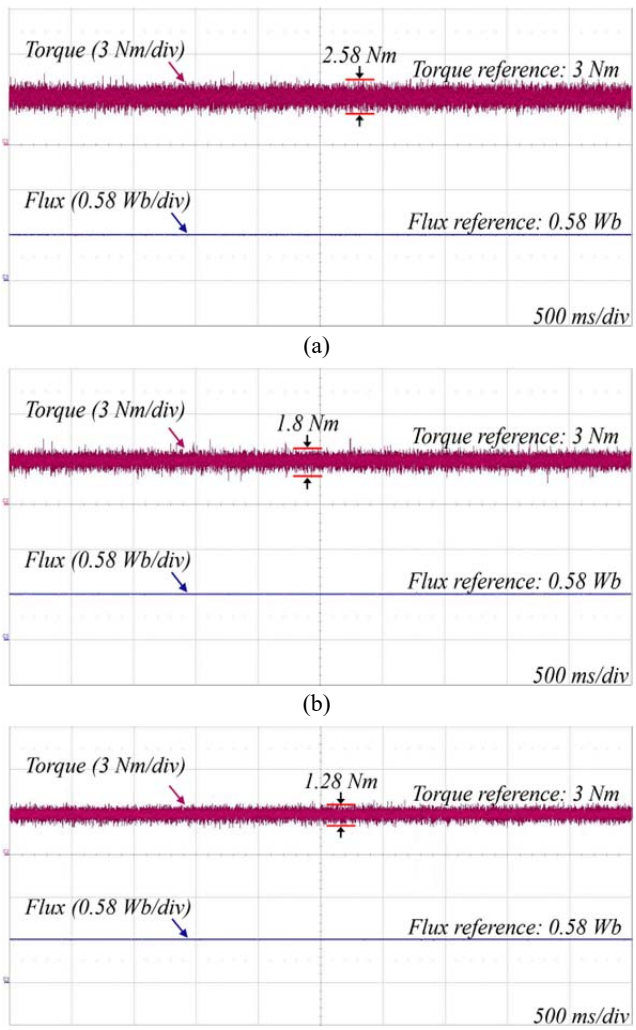

Fig. 11. Experiment results of the torque and flux control using the different voltage vector magnitudes. (a) A large voltage vector. (b) A medium voltage vector. (c) A small voltage vector.

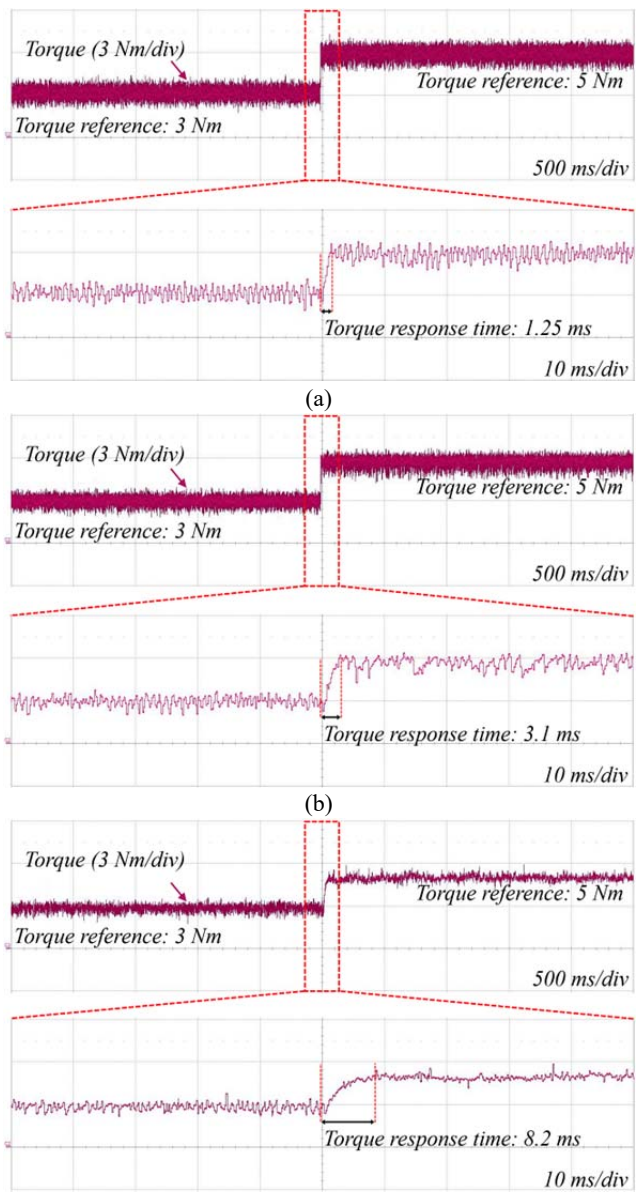

Fig. 12. Experimental results for a change in the torque reference (3 Nm → 5 Nm). (a) A large voltage vector. (b) A medium voltage vector. (c) A small voltage vector.

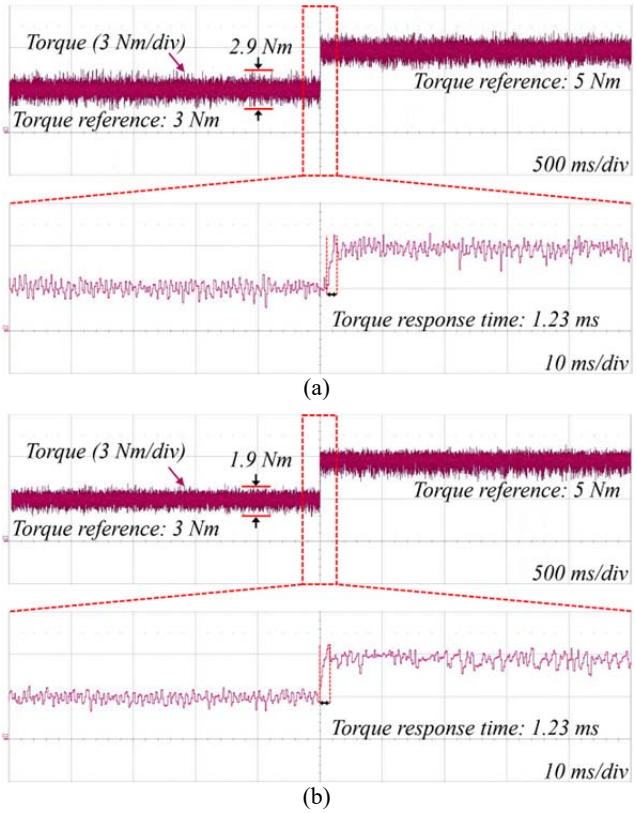

Fig. 13. Experimental results for a change in the torque reference (3 Nm → 5 Nm). (a) Seven-level hysteresis band. (b) Proposed method.

Experimental results for the transient state when the load is changed from 3 Nm to 5 Nm are shown in Fig. 12. The best results in terms of the torque response time are shown in Fig. 12(a), with a response time of 1.25 ms. On the contrary, in Fig. 12(c), the response time is slow with a value of 8.2 ms.

Fig. 13 shows experimental results for both the conventional and proposed methods. Because large voltage vectors are used for both methods, the torque response times are identical. However, the torque ripple is increased with the conventional method because a large voltage vector should be selected in a system with a long control period. With the proposed method, the torque ripple value is much smaller when compared with that of the conventional method. The effectiveness of the proposed method is confirmed by Fig. 13.

V. Conclusion

An improved voltage vector selection algorithm for the DTC of five-phase induction machines is proposed in this paper. The voltage vector of a five-phase inverter has different magnitudes; a large voltage vector has 0.6472 V_{DC}, a medium voltage vector has 0.4 V_{DC}, and a small voltage vector has 0.2472 V_{DC}. The magnitude of the voltage vector is related to the torque ripple and the torque response time. A large voltage vector has the best torque response speed. However, medium and small voltage vectors have less torque ripple. In this paper, a large voltage vector is only selected in the transient state. Meanwhile, medium and small voltage vectors are selected in the steady state. As a result, the torque ripple is reduced in the steady state, and the performance of the torque response speed is improved. The validity of the proposed method is demonstrated through simulation and experimental results.

Acknowledgment

This work was supported by the Korea Institute of Energy Technology Evaluation and Planning(KETEP) and the Ministry of Trade, Industry & Energy(MOTIE) of the Republic of Korea (No. 20174030201660) and by the R&D Program (PK1701B) of the Korea Railroad Research Institute, Republic of Korea.

References

[1] H. A. Toliyat, T. A. Lipo, and J. C. White, "Analysis of a concentrated winding induction machine for adjustable speed drive applications part ii: Motor design and performance," *IEEE Trans. Energy Convers.,* Vol. 6, No. 4, pp. 684-692, Dec. 1991.

[2] G. G. Park, S. H. Hwang, J. M. Kim, K. B. Lee, and D.-C. Lee, "Reduction of current ripples due to current measurement errors in a doubly fed induction generator," *Journal of Power Electronics*, Vol. 10, No. 3, pp. 313-319, May 2010.

[3] K. B. Lee and F. Blaabjerg, "Simple power control for sensorless induction motor drives fed by a matrix converter," *IEEE Trans. Energy Conver.*, Vol. 23, No. 3, pp. 781-788, Sep. 2008.

[4] L. Zheng, J. E. Fletcher, B. W. Williams, and X. He, "A novel direct torque control scheme for a sensorless five-phase induction motor drive," *IEEE Trans. Ind. Electron.*, Vol. 58, No. 2, pp. 503-513, Feb. 2011.

[5] J. A. Riveros, J. Prieto, F. Barrero, S. Toral, M. Jones, and E. Levi, "Predictive torque control for five-phase induction motor drives," in *Proc. 36th Annu. Conf. IEEE Ind. Electron. Soc*., pp. 2467-2472, 2010.

[6] H. A. Toliyat and H. Xu, "A novel direct torque control (DTC) method for five-phase induction machines," in *Proc. IEEE APEC,* pp. 162-168, 2000.

[7] K. B. Lee and F. Blaabjerg, "Performance improvement of DTC for induction motor-fed by three-level inverter with an uncertainty observer using RBFN," *IEEE Trans. Energy Convers.,* Vol. 20, No. 2, pp. 276-283, Jun. 2005.

[8] S. Krim, S. Gdaim, A. Mtibaa, and M. F. Mimouni, "Design and implementation of direct torque control based on an intelligent technique of induction motor on FPGA," *J. Electr. Eng. Technol.*, Vol. 10, No. 4, pp. 1527-1539, Jul. 2015.

[9] W. Song, S. Le, X. Wu, and Y. Ruan, "An improved model predictive direct torque control for induction mechine drives," *Journal of Power Electronics*, Vol. 17, No. 3, pp. 674-685, May 2017.

[10] K. B. Lee and F. Blaabjerg, "Sensorless DTC-SVM for induction motor driven by a matrix converter using a parameter estimation strategy," *IEEE Trans. Ind. Electron.*, Vol. 55, No. 2, pp. 512-521, Feb. 2008.

[11] Y. Cho, K. B. Lee, Y. Lee, and J. Song, "Torque-ripple minimization and fast dynamic scheme for torque predictive

control of permanent-magnet synchronous motors," *IEEE Trans. Power Electron.*, Vol. 30, No. 4, pp. 2182-2190, Apr. 2015.
[12] Y. Cho and K. B. Lee, "Virtual-flux-based predictive direct power control of three-phase PWM rectifiers with fast dynamic response," *IEEE Trans. Power Electron.* Vol. 31, No. 4, pp. 3348-3359, Apr. 2016.
[13] M. D. Islam, C.M.F.S. Reza, and S. Mekhilef, "Modeling and experimental varification of 5-level hybid H-bridge multilevel inverter fed DTC-IM drive," *J. Electr. Eng. Technol.*, Vol. 10, No. 2, pp. 574-585, Mar. 2015.
[14] Q. Yuan, Z. Zeng, and R. Zhao, "Direct stator flux vector control strategy for IPMSM using a full-order state observer," *J. Electr. Eng. Technol.*, Vol. 12, No. 1, pp. 236-248, Jan. 2017.
[15] M. H. Vafaie, B. M. Dehkordi, P. Moallem, and A. Kiyoumarsi, "A new predictive direct torque control method for improving both steady-state and transient-state operations of PMSM," *IEEE Trans. Power Electron.*, Vol. 31, No. 5, pp. 3738-3753, May 2016.
[16] L. Gao, J. E. Fletcher, and L. Zheng, "Low-speed control improvements for a two-level five-phase inverter-fed induction machine using classic direct torque control," *IEEE Trans. Ind. Electron.*, Vol. 58, No. 7, pp. 2744-2754, Jul. 2011.
[17] J. A. Riveros, J. Prieto, F. Barrero, S. Toral, M. Jones, and E. Levi, "Predictive torque control for five-phase induction motor drives," in *Proc. 36th Annu. Conf. IEEE Ind. Electron. Soc.*, pp. 2467-2472, 2010.
[18] Y. N. Tatte and V. A. Mohan, "Torque ripple minimization in five-phase three-level inverter fed direct torque control induction motor drive," in *Proc. EPE'15 ECCE-Europe Conf. IEEE*, pp. 1-6, 2015.
[19] G. H. B. Foo, "Constant switching frequency based direct torque control of interior permanent magnet synchronous motors with reduced ripples and fast torque dynamic," *IEEE Trans. Power Electron.*, Vol. 31, No. 9, pp. 6485-6493, Sep. 2016.
[20] B. Singh, P. Jain, A. P. Mittal, and J. R. P. Gupta, "Torque ripples minimization of DTC IPMSM drive for the EV propulsion system using a neural network," *Journal of Power Electronics*, Vol. 8, No. 1, pp. 23-34, Jan. 2008.
[21] Q. Liu and K. Hameyer, "Torque ripple minimization for direct torque control of PMSM with modified FCSMPC," *IEEE Trans. Ind. Appl.*, Vol. 52, No. 6, pp. 4855-4864, Nov. 2016.
[22] Z. Li, S. Zhang, S. Zhou, and J.-W. Ahn, "Torque ripple minimization in direct torque control of brushless DC motor," *J. Electr. Eng. Technol.*, Vol. 9, No. 5, pp. 1569-1576, Sep. 2014.
[23] Y. N. Tatte and M. V. Aware, "Torque ripple reduction in five-phase direct torque controlled induction motor," in *Proc. Power Electronics, Drives and Energy Systems (PEDES), Conf.*, pp. 1-5, 2014.
[24] L. R. L. V. Raj, A. Jidin, Z. Ibrahim, K. A. Karim, M. A. Said, and M. H. Jopri, "Optimal torque control performance of DTC of 5-phase induction machine," in *Proc. Electrical Machines and Systems (ICEMS), Conf*, pp. 2094-2099, 2013.
[25] S. Y. Kang, H. U. Shin, and K. B. Lee, "Improved torque ripple reduction method of five-phase induction motor using fuzzy controller," in *Proc. IPEMC-ECCE Asia Conf.*, pp. 635-640, 2016.
[26] G. Foo and M. F. Rahman, "Sensorless direct torque and flux-controlled ipm synchronous motor drive at very low speed without signal injection," *IEEE Trans. Ind. Electron.*, Vol. 57, No. 1, pp. 395-403, Jan. 2010.
[27] S. Y. Kang and K. B. Lee, "Improved switching selection for direct torque control of a five-phase induction motor," in *Proc. 2016 ITEC Asia-Pacific Conf.*, pp. 651-655, 2016.

Seong-Yun Kang received his B.S. and M.S. degrees in Electrical and Electronic Engineering from Ajou University, Suwon, Korea, in 2015 and 2017, respectively. Since 2017, he has been with Dawonsys Co., Ltd, Ansan, Korea. His current research interests include motor drives and grid-connected systems.

Hye Ung Shin received his B.S. degree in Electrical and Computer Engineering from Kunsan University, Kunsan, Korea, in 2012; his M.S. degree from the Department of Electronic Systems Engineering of Hanyang University, Ansan, Korea, in 2014; and his Ph.D. degree in Electrical Engineering from Ajou University, Suwon, Korea, in 2017. He has worked for Department of Electric Powertrain R&D, Ssangyong Motor as an Assistant Research Engineer since 2017. His current research interests include machine design, electric machine drives and power conversion.

Sung-Min Park received his B.S. degree in Electronics Engineering and M.S. degree in Electrical Engineering from Korea University, Seoul, Korea, in 2001 and 2003, respectively. He received his Ph.D. from the University of Connecticut, Storrs, CT, USA, in 2015. From 2003 to 2008, he was a Senior Engineer with LG Electronics, Seoul. From 2008 to 2010, he was with Samsung Heavy Industries, Suwon. From 2014 to 2015, he was a Senior Research Engineer at the United Technologies Research Center (UTRC), East Hartford, CT, USA. Since 2015, he has been an Assistant Professor in the Department of Electronic and Electrical Engineering, Sejong, Hongik University. His research interests include power electronics applications for home appliances and renewable energy systems.

Kyo-Beum Lee received his B.S. and M.S. degrees in Electrical and Electronic Engineering from Ajou University, Suwon, Korea, in 1997 and 1999, respectively; and his Ph.D. degree in Electrical Engineering from Korea University, Seoul, Korea, in 2003. From 2003 to 2006, he was with the Institute of Energy Technology, Aalborg University, Aalborg, Denmark. From 2006 to 2007, he was with the Division of Electronics and Information Engineering, Chonbuk National University, Jeonju, Korea. In 2007, he joined the School of Electrical and Computer Engineering, Ajou University, Suwon, Korea. He is an Associate Editor of the *IEEE Transactions on Power Electronics*, the *Journal of Power Electronics*, and the *Journal of Electrical Engineering & Technology*. His current research interests include electric machine drives, renewable power generation, and electric vehicle applications.